Journal of ELECTRICAL ENGINEERING, VOL 70 (2019), NO-7S, 27–35

sciendo

PAPERS

Reliability improvement of electrically active defect investigations by analytical and experimental deep level transient: Fourier spectroscopy investigations

Arpad Kosa*, Beata Sciana, Lubica Stuchlikova***

This article discusses the importance of analytical and experimental approaches in Deep level transient Fourier spectroscopy in terms of reliability, to support the current research and the utilization of this technique for complex investigations. An alternative evaluation approach is proposed and validated by relevant experiments. Attention is focused on a GaAs p-i-n structure, the undoped layer induced defect conduction type statement difficulty, accurate evaluation of a dual type majority-minority carrier defect complex and possible limitations of the DLTS experimental technique. Comprehensive evaluation is carried out and the method is discussed in detail. In comparison with reference data, higher precision of calculated activation energies, differences even lower as 10^{-3} order of magnitude, were achieved.

K e y w o r d s: deep level transient Fourier spectroscopy, Arrhenius data analysis, electrically active defects, GaAs p-i-n, deep energy level

1 Introduction

Progress in semiconductor technology constantly requires new materials and structures to reach higher performances and efficiencies in all technological branches. To optimize the fabrication process, it is essential to study electrical active defects. The deep level transient spectroscopy method (DLTS) founded in 1974 by David Vern Lang [1] is one of the most frequently used diagnostic methods of emission and capture processes investigations in semiconductors. Since the basic methodology was defined, many improvements and measurement systems were developed with a continuous effort to refine the analysis and to achieve highly reliable experiments [2, 3]. Deep energy levels, often described as traps, defect states or impurities are most of the time direct sources of material degradation, undesired electrical, optical or even structural properties. DLTS is used as a standard method in many laboratories and it is capable to identify important defect parameters: the activation energy, capture cross-section and concentration. It is valuable for its sensitivity, which surpasses almost any diagnostic technique. It also detects traps with concentration densities on the order of 10^{-5} cm^{-3} [4]. However, with the right high-sensitivity bridges it can reach values up to 10^{-6} cm^{-3} [5]. Among its other benefits we could highlight the technical simplicity, spectroscopic and non-destructive nature. Despite all these benefits, in complex cases the method can result uncertain results, and difficulties in interpretations. Indispensable part of DLTS investigation is the utilization and comparison of various methods, analytical procedures and reference data. Different structural, material, composition factors are needed to be considered to establish a reliable diagnosis. Even a spectrum with a significant peak is measured, it is not estimable. In some cases, even the opposite could be true, trap parameters are calculated with high reliability, but structural parameters are indicating a questionable result [6, 7].

This article discusses an alternative analytical deep level transient Fourier spectroscopy study to achieve reliable electrically active defect parameters of complex spectrums. Results are supported by experiments and compared to different evaluation methods.

1.1 Deep level transient spectroscopy

The DLTS method is based on measurements of capacitance differences caused by emission and capture processes of charge carriers. This is achieved by various excitation sources and the changing depletion region of the semiconductor barrier structure. More precisely, the measured sample needs to be contacted with a metal layer to form a rectifying metal – semiconductor junction (Schottky barrier) or with another semiconductor to form a p-n junction. Space charge region is created in the proximity of the contact.

The best way to illustrate DLTS principles is to explain Lang's basic capacitance DLTS with a voltage excitation pulse (Fig. 1). While the reverse bias U_R is applied

*Institute of Electronics and Photonics, Faculty of Electrical Engineering and Information Technology, Slovak University of Technology, Ilkovicova 3, Bratislava, Slovakia, arpad.kosa@stuba.sk, **Division of Microelectronics and Nanotechnology, Faculty of Microsystem Electronics and Photonics, Wroclaw University of Science and Technology, Janiszewskiego 11/17, Wroclaw, Poland,

DOI: 10.2478/jee-2019–0038, Print (till 2015) ISSN 1335-3632, On-line ISSN 1339-309X

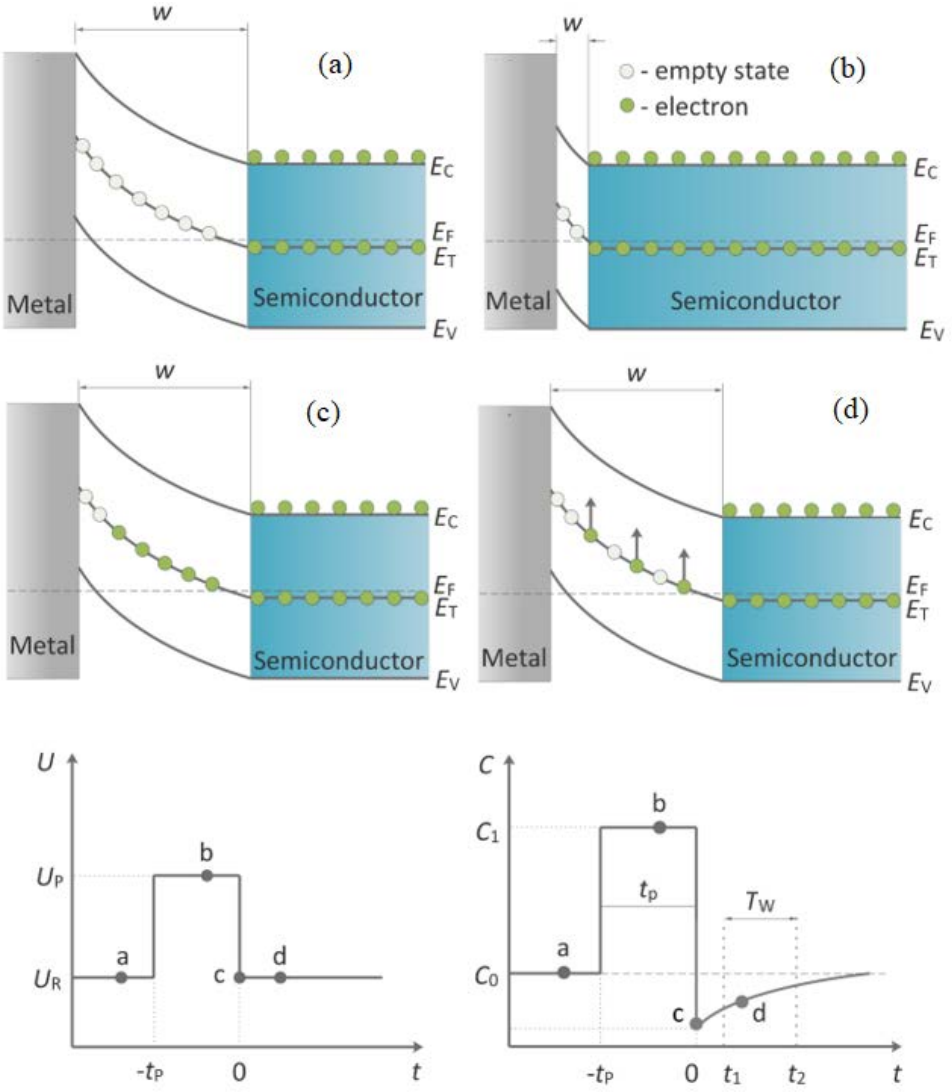

Fig. 1. Principles of the DLTS method

on the structure, the capacitance of the space charge region is C_0. Traps that are located above the Fermi level are empty, Fig. 1(a). When the filling pulse U_P is applied, the depletion region width shortens, and the capacitance rises. The defect state captures electrons (or holes), Fig. 1(b). After filling pulse elapses (time t_P), the voltage is again reduced to the reverse bias value U_R, Fig. 1(c). Carriers are emitted back to conduction (or valence) band via thermal emission. This process results an exponential capacitance change with an emission ratio described as the reciprocal value of emission time constant τ, Fig. 1(d). After a certain period (T_W) the capacitance settles again at the value C_0, hence it returns to thermodynamic equilibrium. This process is repeated at different temperatures at which the capacitance transient signals are measured [8]. The transient signal is then processed by various mathematical procedures, *eg* Fourier or Laplace transformation as an enhancement of the basic DLTS method. In the basic approach the values of capacitance transient signal at times t_1 and t_2 (so called rate window RW) are subtracted from the relation $\Delta C(T) = C(t_1) - C(t_2)$. This difference ΔC is temperature dependent, thus a spectrum ΔC *vs* T can be calculated. By shifting the rate window, several spectrums are obtained which describe the defect's peak activity.

As the emission time constant is dependent on the temperature, increasing-decreasing differences in capacitance changes are outlined, and in the same time, a peak in the spectrum is observed [9]. Each peak in the spectrum is indicating the presence of an electrically active defect, which is also calculated as an Arrhenius curve (effects of temperature on emission).

The Arrhenius equation $\ln(\tau\nu_{\mathrm{th}}N_{\mathrm{C,V}}) = \frac{\Delta E}{k}\frac{1}{T} - \ln(X_{\mathrm{n,p}}\sigma_{\mathrm{n,p}})$ is defined using the emission time constant, the thermal velocity ν_{th} and density of states $N_{\mathrm{C,V}}$. This relation can be described as the exponentially changing charge carrier concentration on the defect

state during emission or capture for the specific temperature. The following equation is valid: $\nu_{\mathrm{th}} = \sqrt{\frac{3kT}{m^*_{\mathrm{n,p}}}}$ and $N_{\mathrm{C,V}} = 2M\left(\frac{2\pi m^*_{\mathrm{n,p}} kT}{h^2}\right)^{\frac{3}{2}}$ where $m^*_{\mathrm{n,p}}$ is the effective mass of electrons or holes. The $X_{\mathrm{n,p}}$ is the entropy factor of electrons or holes, M the number of equivalent minimums of the valence band, k is the Boltzmann and h the Planck constant. From the analogy of the above equations and the linear regression the main parameters of the defect states (activation energy ΔE_{T} and capture cross section σ_{T}) can be obtained: $\ln(\tau\nu_{\mathrm{th}}N_{\mathrm{C,V}}) = A\frac{1}{T} - B$. The activation energy ΔE_{T}, can be calculated from the slope of the regression line: $\Delta E_{\mathrm{T}} = Ak$, while the capture cross-section σ_{T} can be calculated from the intercept: $\sigma_{\mathrm{n}} = \frac{\exp(B)}{X_{\mathrm{n,p}}}$ [10-12].

Digital signal processing using the Fourier transform achieved a major importance in many systems including DLTS and made possible to improve the classical DLTS method. Deep Level Transient Fourier Spectroscopy was defined, which allows a completely computer controlled measurement, separation of overlapped defect states and adjustment of capacitance transients period width scanned in evenly distributed sampling intervals N. From these values discrete Fourier coefficients c_{n} are formed by numerical Fourier transformation, used to calculate the emission time constant τ and amplitude of each capacitance transient signal with period width T_{W}. Since relations between coefficients are characteristic for different signal forms a simultaneous examination of the result is possible giving a great advantage for DLTFS with respect to signal noise ratio. The new approach also makes possible to extend the conventional DLTS rate window determination. Instead of calculating the difference of two transient points a correlator is used, which relates the transient to weighting functions such as rectangle, sine, cosine or exponential, and makes possible to retrieve the Arrhenius curve (Maximum evaluation) [10-12]. Figure 2 shows the correlation between a complex spectrum and capacitance transient signals calculated by the sine function. The peak around 103.5 K shows the amplitude, hence the highest capacitance difference.

In the DLTFS method Arrhenius curves are defined by direct and indirect evaluation methods. The indirect maximum evaluation method relies only on DLTFS spectra, while direct Arrhenius curves are calculated based on capacitance transient signals and their parameters. The most important of these is the evaluation class, which is defined by the quality of the transient for *eg* by signal to noise ratio. Literature [10-12] defines this parameter to be minimally 40 to get acceptable results. It is evident that highly classified transient signals are located around DLTFS peak maximums and minimums and are sources of most significant data. The direct evaluation method also includes a mathematical separation, an ideal tool for deconvolution of composite DLTFS spectrums. In this case it is assumed that the resulted DLTFS spectrum contains responses from more than one defect where further analysis is needed.

Regardless the advantage of DLTFS in deconvolution, it is necessary to support the DLTFS experiments by other techniques such as the Minority Carrier DLTFS, which allows us to excite only minority carrier emission by illumination, thereby to filter these responses from a complex DLTFS spectrum.

Table 1. Geometrical properties of the investigated GaAs p-i-n structure

Layer	Thickness d (nm)	Concentration $p,\ n$ (cm^{-3})
p^+-GaAs:Zn Cap	50	$1 \div 3 \times 10^{19}$
p-GaAs:Zn	200	$2 \div 3 \times 10^{18}$
i-GaAs	200	–
n gradient GaAs	800	$2 \div 3 \times 10^{18}$ to $1 \div 2 \times 10^{17}$
n-GaAs Buffer	200	$1 \div 3 \times 10^{18}$
n-GaAs:Si substrate	–	$2 \div 3 \times 10^{18}$

1.2 The experimental setup and sample preparation

DLTFS experiments were realized by the measurement system BIORAD DL8000, equipped with liquid nitrogen cooling and two excitation methods: electrical and optical. The system is capable to maintain temperatures from 85 K to 550 K and measure capacitance transients for multiple measurement sets at once. Capacitance is measured by Boonton 72B capacitance meter using a high frequency signal with 100 mV amplitude, and 1 MHz frequency. By software regulation, it can measure capacitance up to 3000 pF in 4 ranges. The measured structures are placed in a cryostat with vacuum conditions to avoid any environmental measurement dependencies.

To analyse the DLTFS evaluation possibilities a GaAs p-i-n sample was examined. The structure was grown by Atmospheric Metal Organic Vapour Phase Epitaxy (AP-MOVPE) using an AIX 200 R&D horizontal reactor on n-type GaAs (Si doped) substrates at the Wroclaw University of Science and Technology. As n-type and p-type dopant sources silane (SiH_4: 20 ppm mixture in H_2) and diethylzinc (DEZn, ($Zn(C_2H_5)_2$) were used, respectively. High purity hydrogen was utilized, as carrier gas (99.9999%). Trimethylgallium (TMGa, ($Ga(CH_3)_3$)) and arsine (AsH_3: 10% mixture in H_2) with flow rates $V_{\mathrm{TMGa}} = 10$ ml/min and $V_{\mathrm{AsH3}} = 300$ ml/min were applied as growth precursors at a growth temperature of 670 °C [13]. The carrier concentration in n-type and p-type epilayers was estimated using Bio-Rad 4300 electrochemical capacitance-voltage (EC-V) profiler. The metallization was prepared by deposition on the top and bottom side of the structure with p-type AuBe transparent and n-type AuGeNi standard layers. The transparency was determined as 40%. Geometrical parameters are listed in Tab 1.

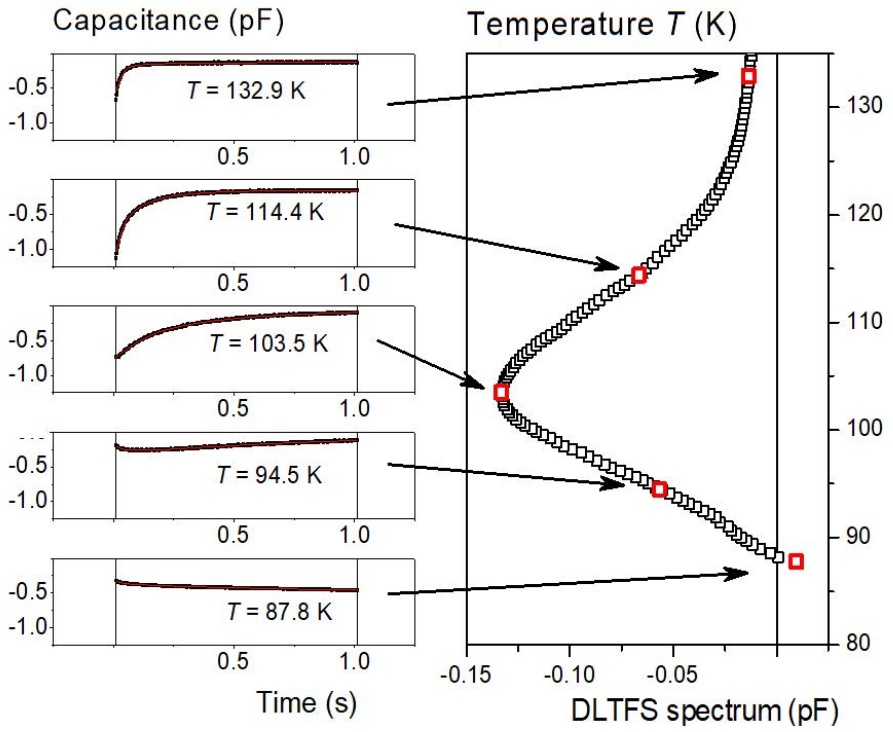

Fig. 2. Example of the DLTS spectrum and capacitance transient signals: $T_w = 1$ s, $U_p = 0.05$ V, $U_R = -0.5$ V, $t_p = 300$ ms

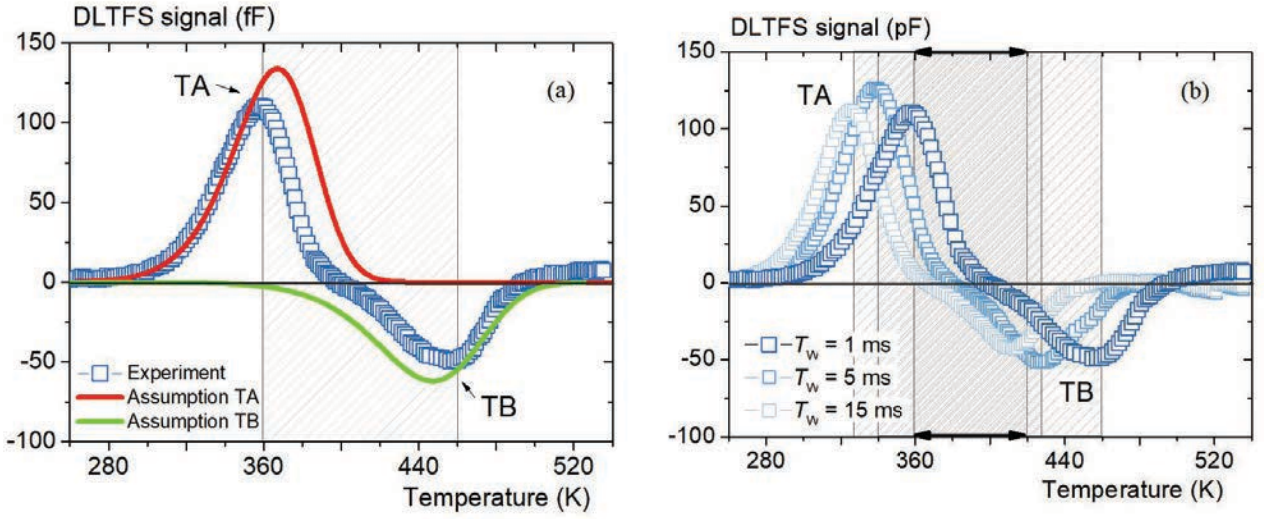

Fig. 3. DLTFS of GaAs p-i-n, $U_p = 0.05$ V, $U_R = -0.5$ V, $t_p = 3$ ms, with assumed curve origins: (a) – $T_w = 1$ ms, and (b) – transition areas

2 Challenges of DLTFS

One of the most difficult parts of the DLTFS method is the interpretation of experimental results. Reliability of the method is mainly affected by complex situations, in which different defect states are interacting. It is hard to precisely deconvolute these spectrums and to calculate relevant Arrhenius curves. To improve the DLTFS reliability a variety of analytical and experimental investigations are needed to be compared and assessed. Moreover, reverse simulations are also necessary to extend the analysis and approve the obtained results. A good example on this is the GaAs p-i-n semiconductor structure, often used in multilayer solar cell samples to improve the generation of free charge carriers [14]. Since in this case depletion region is located at the undoped region and the conduction type is not exact, the defect carrier assignment is not obvious. It is difficult to state the proper type (p or n) of

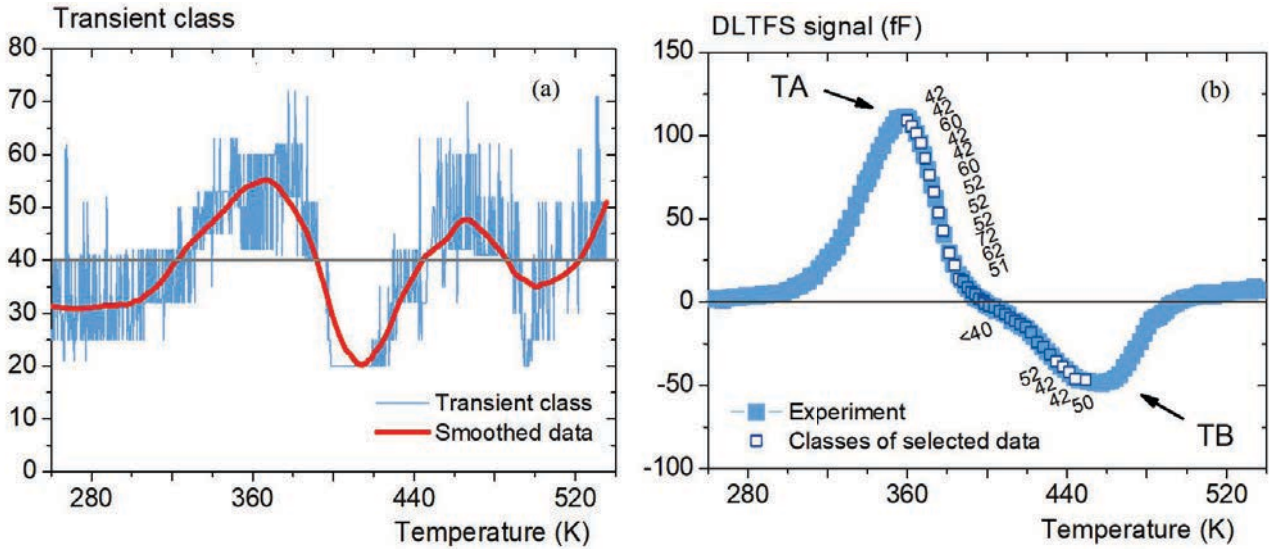

Fig. 4. Transient classifications of the GaAs p-i-n DLTFS spectrum, $T_{\mathrm{w}} = 1$ ms, $U_{\mathrm{p}} = 0.05$ V, $U_{\mathrm{R}} = -0.5$ V, $t_{\mathrm{p}} = 3$ m

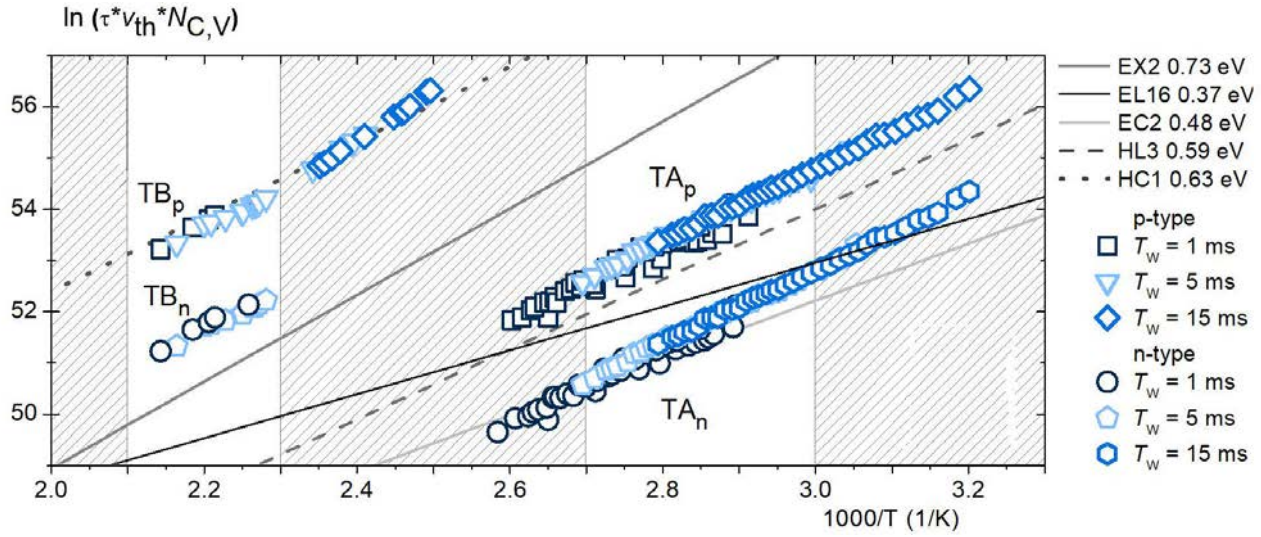

Fig. 5. Arrhenius curves of the GaAs p-i-n sample: $U_{\mathrm{p}} = 0.05$ V, $U_{\mathrm{R}} = -0.5$ V, $t_{\mathrm{p}} = 3$ ms

observed defects [15]. In case of DLTFS spectra, a sharp drop between a positive and negative peak is also typical complicating the investigation, Fig. 3(a). If this situation is examined more closely by adding an assumed spectral origin for trap states TA and TB, Fig. 3(a), we can assume that a possible complex defect interaction is capable to reduce and shift the spectrum. To sort out unreliable data of such a result, a region of spectrum transition must be defined (Fig. 3 shaded). In addition, this region needs to be applied to all experimental results within a period set. Overlapping transition regions are indicating a highly avoidable area as evaluation data sources Fig. 3(a) right.

Since each transient signal represents one point in the spectra, specific evaluation classes around these regions can be examined. The next two figures are showing these values for all measured data and selected points of the transition area (Fig. 4). To properly visualize these data a smoothed curve was added to the first figure, which shows the character of the signal. Two approximate ranges of correct evaluation data, in the ranges 330 – 380 K and 440 – 480 K can be defined. Here the class reaches 50 and higher values. It is evident that many points in the transition-avoidable area are located above the 40-limit, thus it is included in the standard evaluation process. According to our assumption, precisely these data are degrading the evaluation reliability and all the selected data below 40 should be avoided.

For undoped layers it is also necessary to evaluate the measured data for both p- and n-type, since effective masses for electrons and holes are used in the Arrhenius calculations [15]. In comparison with available referent data [16-19] the results show shifted Arrhenius curves located in the transition or in other words avoidable areas. Fig. 5 shows Arrhenius curves of majority and minority

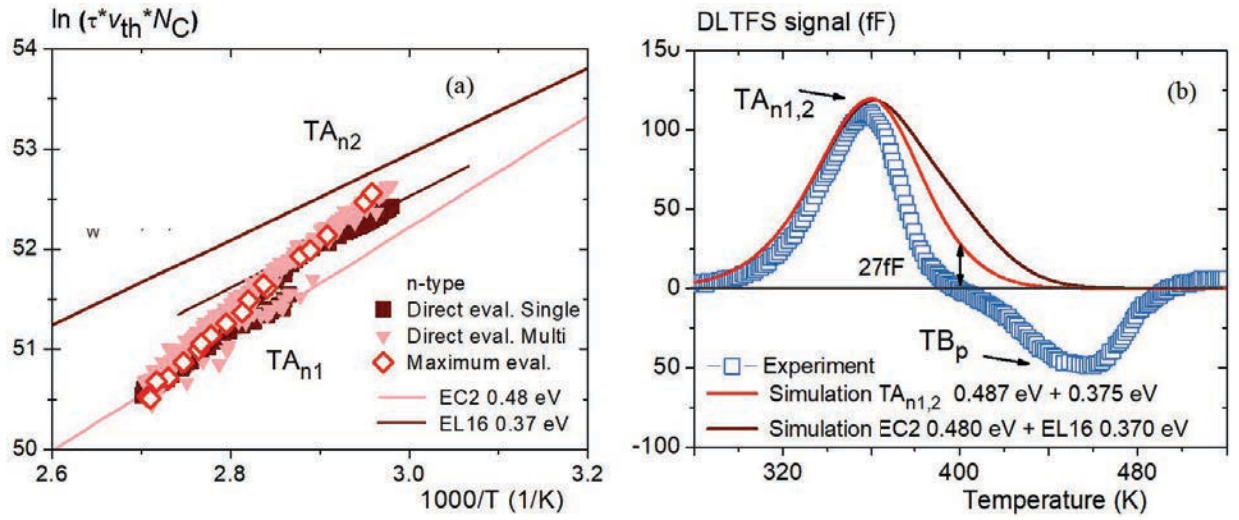

Fig. 6. Arrhenius of $TA_{n1,2}$, $U_p = 0.05$ V, $U_R = -0.5$ V, $t_p = 3$ ms, (a) – with measured $T_w = 1, 5, 15$ ms, and (b) – simulated DLTFS curves $T_w = 1$ ms

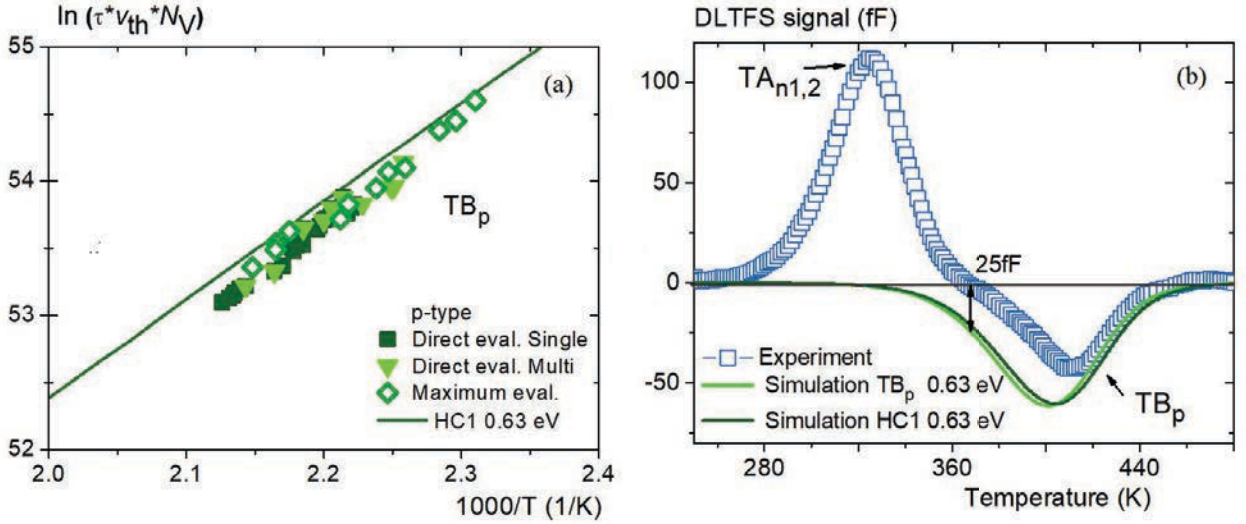

Fig. 7. Arrhenius of TB_p , $U_p = 0.05$ V, $U_R = -0.5$ V, $t_p = 3$ ms, (a) – with measured $T_w = 1, 5, 15$ ms, and simulated DLTFS curves $T_w = 15$ ms, and simulated DLTFS curves(b) – $T_w = 15$ ms

trap responses TA and TB calculated by Direct evaluation - deconvolution for both p and n type n-type (scatter) compared with references (lines).

3 Analytical DLTFS evaluation approach of reliable defect detection

As described, to ensure a precise Arrhenius curve calculation, we need to eliminate all possible sources of unwanted data, not sorted by the regular evaluation. The proposed analysis was aimed to select these data and recalculate deep energy level parameters by available methods, and to validate by simulations.

The approach revealed a complex defect state in the case of TA ($TA_{n1,2}$) after data sorting. As Fig. 6 shows, more precise Arrhenius points and the evidence of a mutually interacting defect complex was observed. Sorted Arrhenius curves of the complex defect state $TA_{n1,2}$ with referent data EC2 + EL16, Fig. 6(a), supported this statement. Measured and simulated DLTFS curves of $TA_{n1,2}$ and referent EC2 + EL16 trap levels were also compared, Fig. 6(b). Results for the n-type variant showed higher correspondences with references, a more probable n-type was assumed. This example clearly describes differences of each evaluation method and reliability of calculated defect parameters (Tab. 2). Highly corresponding curves were obtained for trap level TA_{n1} in the case of direct evaluations (filled square and triangle). Defect convolution made possible to state defect parameters also for TA_{n2}, whereas the maximum evaluation process was not able to distinguish between these two responses (not filled square). The proposed data selection method made possi-

Table 2. Defect parameters calculated by the proposed Arrhenius data sorting approach

Label	Method	ΔE_T (eV)	σ_T (cm^2)	ΔE_{Tref} (eV)	σ_{Tref} (cm^2)	Ref.	$\lvert\Delta E_T - \Delta E_{Tref}\rvert$ (eV)
TA_{n1}	Electrical not sorted	0.452	1.46×10^{-16}	0.48 (EC2)	3.8×10^{-16}	Ni [16]	0.028
TA_{n1}	Electrical Sorted	0.488	4.68×10^{-16}	0.48 (EC2)	3.8×10^{-16}	Ni [16]	0.008
TA_{n2}	Electrical not sorted	0.395	1.41×10^{-17}	0.37 (EL16)	4.0×10^{-18}	[17]	0.025
TA_{n2}	Electrical Sorted	0.366	5.57×10^{-18}	0.37 (EL16)	4.0×10^{-18}	[17]	0.004
TB_p	Electrical not sorted	0.691	1.06×10^{-15}	0.63 (HC1)	4.0×10^{-17}	Zn/Ni [18]	0.061
TB_p	Electrical Sorted	0.631	4.76×10^{-15}	0.63 (HC1)	4.0×10^{-17}	Zn/Ni [18]	0.001

Table 3. Defect parameters calculated by the proposed Arrhenius data sorting approach

Label	Method	ΔE_T (eV)	σ_T (cm^2)	ΔE_{Tref} (eV)	σ_{Tref} (cm^2)	Ref.	$\lvert\Delta E_T - \Delta E_{Tref}\rvert$ (eV)
TB_p	Electrical not sorted	0.691	1.06×10^{-15}	0.63 (HC1)	4.0×10^{-17}	Zn/Ni [18]	0.061
TB_p	Electrical Sorted	0.631	4.76×10^{-17}	0.63 (HC1)	4.0×10^{-17}	Zn/Ni [18]	0.019
TB_p	Optical	0.615	2.28×10^{-17}	0.63 (HC1)	4.0×10^{-17}	Zn/Ni [18]	0.015
TC_p	Optical	0.525	5.73×10^{-16}	0.519 (HL8)	3.5×10^{-16}	Fe [21]	0.006

ble to calculate more precise activation energies and capture cross sections. The highest precision was achieved by deconvolution and data selection approach where only 0.001 eV and 0.005 eV energy differences were calculated. The investigation process approved the presence of EC2 (0.48 eV, 3.8×10^{-16} cm^2) and EL16 (0.375 eV, 4.0×10^{-18} cm^2) with high precision (TA_{n1} 0.487 eV, 4.18×10^{-16} cm^2 and TA_{n2} 0.375 eV, 6.94×10^{-18} cm^2). The result was approved also by DLTFS spectra simulation where the assumed peak maximum shift of Fig. 3 (right) was visible.

In this case, the estimation of a proper defect concentration (peak height) is very difficult. If the amplitude of the measured spectrum is affected by the interaction, we can't really assign the simulation to the measured peak amplitude. That is the reason why the simulation was realized in such a way that the estimated curve corresponds to the rising edge of the positive peak where possible influence of the interaction is the lowest. The joined simulation of the $TA_{n1,2}$ complex showed a 27 fF difference 0 fF and around 400 K (Fig. 6 right). The difference should be reduced to zero after the negative peak influence is subtracted.

In case of the deep energy level TB_p a single possible p-type level HC1 (0.63 eV, 4.0×10^{-17} cm^2) was observed and approved by sorted Arrhenius curves, Fig. 7(a). Measured and simulated DLTFS curves of calculated TB_p and referent HC1 trap levels, Fig. 7(b), were also included. For this case spectrum simulation was realized according to the rising edge of negative spectrum. The difference at 0 fF and around 380 K between the measured and simulated spectrum was 25 fF, Fig. 7(b).

If each obtained difference (27 fF and 25 fF) is subtracted, we get a 2 fF result, indicating that the interacting evaluated defects and the simulated curves can in fact have the experimentally measured result.

4 Experimental DLTFS approaches of a reliable defect detection

Key step in DLTFS investigation of complex defect states is the deconvolution process. The deconvolution is achievable by the evaluation process, however it is not fully reliable. In some cases, this interaction can be filtered out also by experimental approaches. These include DLTFS measurement parameter variations with electrical excitation pulses optimized to achieve separate spectrums, although this process is time consuming and not definite. A suitable, more effective solution is the utilization of Minority Carrier Deep Level Transient Fourier Spectroscopy (MCDLTFS) with optical and combined excitation impulses. The conventional DLTFS excitation is realized by electrical pulses, while minority carrier traps can be observed when the excitation process is replaced by appropriate light pulses [19]. According to the theory, a proper wavelength laser interacting with minority carriers and the valence band can filter out the majority response [20]. In our case, a GaAs ($E_G = 1.424$ eV) laser with $P = 100$ mW maximum power and near infrared wavelength $\lambda = 850$ nm was used.

As it was desired, the optical excitation made possible to filter out the $TA_{n1,2}$ complex, Fig. 8(a) and to ensure a more reliable evaluation of the TB level, Fig. 8(b). Additionally, this approach made possible to identify minor-

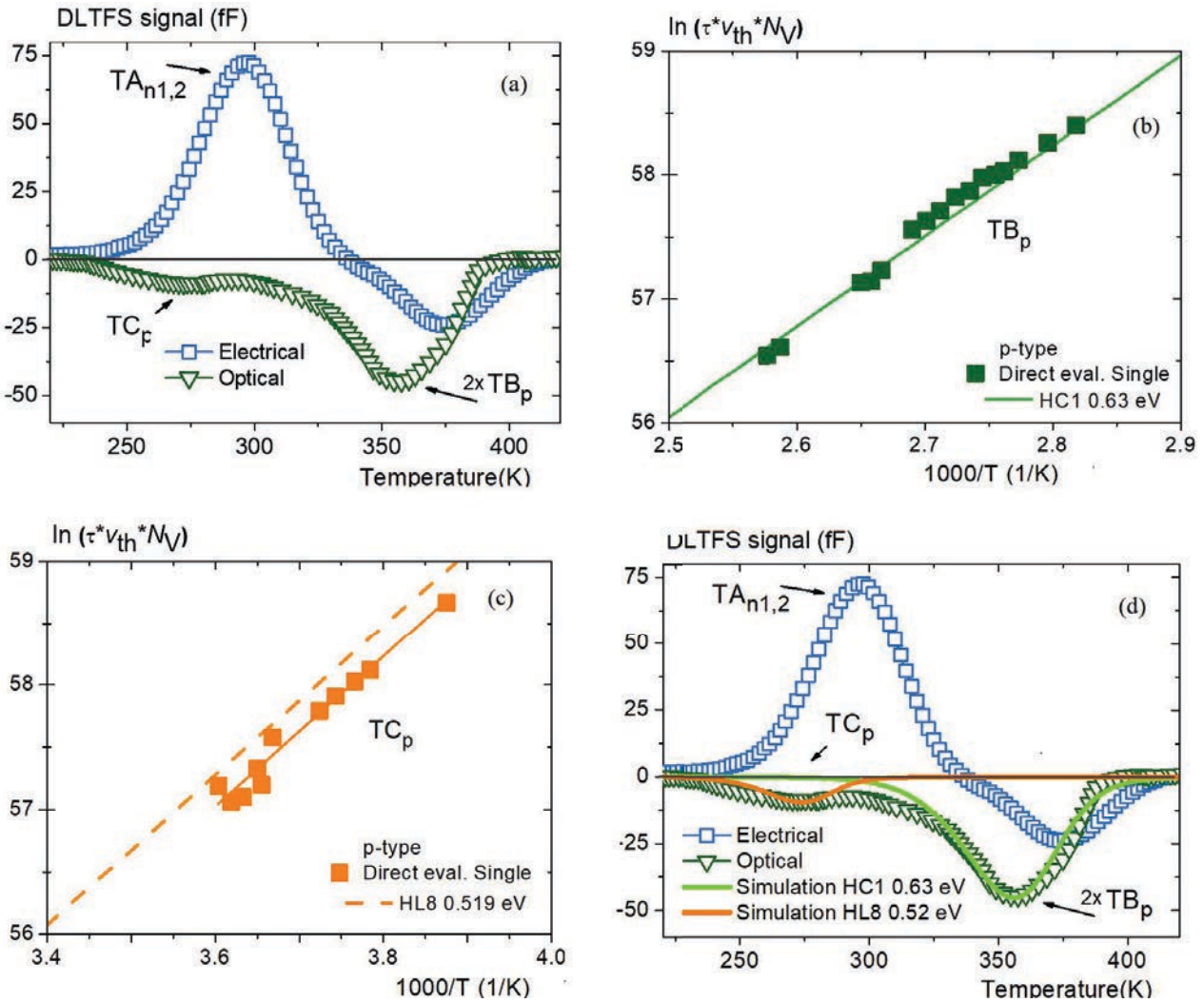

Fig. 8. Comparison of standard DLTFS and MCDLTFS measurements of GaAs p-i-n: $U_R = -0.5$ V, $U_p = 0.05$ V, $t_{po} = 10$ ms, (a),(d) – $T_w = 0.2$ s, (b),(c) – $T_w = 0.2, 0.5, 1$ s

ity trap level with temperatures near $TA_{n1,2}$, which was not visible in the initial spectrum, Fig. 8(c) TC_p. Figure 8(a) documents the comparison of standard DLTFS and MCDLTFS measurements, (b), (c) Arrhenius curves of minority trap responses TB_p and TC_p and d) simulations of reference deep energy levels HC1 and HL8. If the MCDLTFS spectrum is closely examined we can conclude, that the assumption of a possible shifted spectrum origin of Fig. 3 was confirmed experimentally. Origin of the deep energy level TB_p with activation energy $\Delta E_T = 0.615$ eV was once again confirmed by this experimental approach. Reference defect level HC1 ($\Delta E_{Tref} = 0.615$ eV) was stated. These experiments also revealed traces of a new trap level, labelled as TC_p ($\Delta E_T = 0.53$ eV), which was identified according to literature as HL8 ($\Delta E_{Tref} = 0.52$ eV). The validity of the evaluation was also controlled by reverse DLTFS simulations. Two curves were simulated by reference data HC1 and HL8 assigned to the MCDLTFS spectrum. As Fig. 8(d) shows, these results were in good agreement with the obtained experimental data. The assessed results of identified activation energies in comparison with references approved, that the introduced data selection approach was correct , see Tab. 3. The lowest energy differences were observed for the optical and the proposed analytical method.

As this specific case shows, to investigate a defect interaction, a complex approach is needed to ensure reliable defect parameter calculation. Data sorting and defect parameter recalculation is a promising option to solve this task.

5 Conclusion

The discussed analysis deals with a comprehensive DLTFS investigation in terms of reliability improvement of a dual type majority-minority carrier undoped GaAs defect complex evaluation. An alternative analytical approach of Arrhenius data sorting was proposed, tested

and validated, to overcome standard DLTFS evaluation limitations and to ensure a more precise deep energy level parameter calculation. In comparison with reference data, higher precision of calculated were achieved, with activation energy differences even lower as 10^{-3} order of magnitude. Defect interaction and assumed effects on DLTFS spectra, hence shifting peak positions and reduced amplitudes were confirmed experimentally by Minority carrier DLTFS and spectrum simulations. The realized high precision defect investigation showed two dominant defect states of the dual type complex with activation energies at 0.48 eV and 0.63 eV, connected to a possible growth process source.

The aim of this work was to propose an alternative evaluation approach of complex deep energy level analysis which faces various challenges and tasks during realizations. As the result of this discussion, we can conclude, that the utilization of various DLTFS defect recognition techniques, as well as analytical approaches is a crucial must in complicated structure analysis.

Acknowledgements

This work has been supported by the Scientific Grant Agency of the Ministry of Education of the Slovak Republic (VEGA 1/0668/17) and by the Slovak Research and Development Agency (APVV-15-0152). This work was co-financed by Wroclaw University of Science and Technology statutory grants.

References

[1] D. V. Lang, "Deep-levellevel transient spectroscopy: A new method to characterize traps in semiconductors", *Journal of Applied Physics*, vol. 45.7, pp. 3023–3032, 1974.

[2] A. Kosa, L. Stuchlikova, W. Dawidowski, J. Jakus, B. Sciana, D. Radziewicz, D. Pucicki, L. Harmatha, J. Kovac, M. Tlaczala, "DLTFS Investigation of Ingaasn/Gaas Tandem Solar Cell", *Journal of Electrical Engineering*, vol. 65(5), pp. 271–276, 2014.

[3] L. Harmatha, M. Mikolasek, L. Stuchlikova, A. Kosa, M. Ziska, L. Hrubcin, V. A. Skuratov, "Electrically active defects in solar cells based on amorphous silicon/crystalline silicon heterojunction after irradiation by heavy Xe ions", *Journal of Electrical Engineering*, vol. 99, pp. 323–328, 2015.

[4] D. K. Schroder, *Semiconductor material and device characterization, 3rd ed.*, N. J. Hoboken, Wiley, 779, 2006, ISBN 9780471739067.

[5] S. Misrachi, A. R. Peaker, B. Hamilton, "A high sensitivity bridge for the measurement of deep states in semiconductors", *Journal of Physics E: Scientific Instruments*, vol. 13(10), pp. 1055–1061, 1980.

[6] A. Kosa *et al*, "Defect distribution in InGaAsN/GaAs multilayer solar cells", *Solar Energy*, vol. 132, pp. 587–590, 2016.

[7] L. Stuchlikova *et al*, "Electrical Characterization of the AII-IBV-N Heterostructures by Capacitance Methods", *Applied Surface Science*, vol. 269, pp. 175–179, 2013.

[8] S. Weiss, R. Kassing, "Deep Level Transient Fourier Spectroscopy (DLTFS) - A technique for the analysis of deep level properties", *Solid-State Electronics*, vol. 31(12), pp. 1733–1742, 1988.

[9] W. Shockley, W. T. Read, "Statistics of the Recombinations of Holes and Electrons", *Physical Review*, vol. 87(5), pp. 835–842, 1952.

[10] PhysTech, "Deep-Level Transient Spectroscopy System", Theory Manual, Online: www.phystech.de, 2010.

[11] PhysTech, "Deep-Level Transient Spectroscopy System", Software Manual, Online: www.phystech.de, 2010.

[12] PhysTech, "Deep-Level Transient Spectroscopy System", Software Basics, Online: www.phystech.de, 2010.

[13] W. Dawidowski, *et al*, "AP-MOVPE technology and characterization of InGaAsN pin subcell for InGaAsN/GaAs tandem solar cell", *International Journal of Electronics and Telecommunications*, vol. 60(2), pp. 151–156, 2014.

[14] R. Tony, "Special purpose diodes, All about circuits", Online: www.allaboutcircuits.com, 2012.

[15] J. Toompuu, *et al*, "Investigation of deep level centers in i-and n-layers of GaAs pin-diodes", *14th Biennial Baltic Electronic Conference (BEC), IEEE*, pp. 25–28, 2014.

[16] A. Babinski, M. Baj, A. M. Hennel, "The pressure dependence of transition metal-related levels in GaAs", *Acta Physica Polonica A*, vol. 79(3), pp. 323, 1991.

[17] O. Engstrom, M. Kaniewska, "Discovery of classes among deep level centers in gallium arsenide", *Materials Science and Engineering B*, vol. 138(12), pp. 12–15, 2007.

[18] D. L. Partin, *et al*, "Defect Formation in GaAs by Subthreshold Energy (0.2 – 3 keV) Electron Irradiation", *Journal of Applied Physics*, vol. 50, pp. 6845, 1979.

[19] M. Takikawa; T. Ikoma, "Photo-excited DLTS: Measurement of minority carrier traps", *Japanese Journal of Applied Physics*, vol. 16(7), 1980.

[20] J. H. Evans-Freeman, M. A. Gad, "High resolution minority carrier transient spectroscopy of defects in Si and Si/SiGe quantum wells", *Physica B: Condensed Matter*, vol. 308, pp. 554–557, 2001.

[21] P. Dobrilla, "Stoichiometry related deep levels in undoped, semi-insulating GaAs", *Journal of applied physics*, vol. 64(12), pp. 6767–6769, 1988.

Received 19 March 2019